ELSEVIER

Journal of Alloys and Compounds 356–357 (2003) 252–257

Journal of ALLOYS AND COMPOUNDS

www.elsevier.com/locate/jallcom

Tunneling of H within nearly undistorted substitutional-H pairs in Nb: a centrosymmetric four-level system

F. Cordero[a,c,*], A. Paolone[b,c], R. Cantelli[b,c]

[a]*CNR, Area della Ricerca di Roma-Tor Vergata, Istituto di Acustica 'O.M. Corbino', Via del Fosso del Cavaliere 100, I-00133 Roma, Italy*
[b]*Università di Roma 'La Sapienza', Dipartimento di Fisica, P.le A. Moro 2, I-00185 Roma, Italy*
[c]*INFM, Roma, Italy*

Received 1 June 2002; accepted 26 October 2002

Abstract

The geometry and dynamics of the tunnel systems of H trapped by substitutional atoms in Nb has been studied by anelastic spectroscopy on very diluted $NbZr_y(H/D)_x$ alloys ($x<y<0.0015$). At such low impurity levels the features of the anelastic spectrum of the nearly non-interacting complexes are observable, and finally provide clear evidence of the delocalization of H in centrosymmetric four-level systems (FLS). An additional process is found at liquid He temperatures, besides that present also at higher concentrations, and similar to the anelastic response of a two-level system. The new process has an intensity that does not vanish for small asymmetries and a slow rate dominated by two-phonon transitions. Such features can be easily explained in terms of a simple perturbative approach, in which the transitions with the intermediate energy levels of a FLS turn out to be prohibited in the first order.

Keywords: H delocalization; Anelastic spectroscopy; Transitions of multi-level systems

1. Introduction

The tunneling of H trapped near interstitial (O, N, C) or substitutional (S=Ti, Zr) impurities in Nb, Ta and V has been the object of several experimental and theoretical investigations (Ref. [1] and references therein). The case of the O–H pair is well understood in terms of a two-level system (TLS) with prevalent non-adiabatic interaction with the conduction electrons [1–3]. Instead, in the case of the more symmetric S–H pairs, several indications have been obtained of H delocalization over the four tetrahedral (T) sites of a face of the cube enclosing the S atom, forming a centrosymmetric four-level system (FLS, see Fig. 2 later). However, no experiment was conclusive and other geometries have also been proposed: an anelastic experiment on a Nb single crystal with 2 at% Ti indicated overbarrier jumps between tunnel systems of H delocalized over pairs of T sites across different cube faces [4]. Inelastic neutron scattering (INS) measurements of the excited states of H trapped by Ti in Nb exhibit a complex structure that is evidence of a multi-level tunnel system, compatible with a FLS but also for example with a ring of six T sites [5].

Here we present results of anelastic spectroscopy measurements on highly diluted $Nb_{1-x}Zr_x$ single crystals, where the interactions among the impurities are low enough that the relaxation processes of the nearly unperturbed complexes can be clearly observed. It turns out that such tunnel systems are indeed centrosymmetric FLS, and both the complex phenomenology and the indications of different geometries at higher concentrations result from the severe distortions of the trapping environments.

2. Experimental

The $Nb_{1-x}Zr_x$ samples, with $x=0.0045$ and 0.0013, were single crystal bars approximately $2\times3\times50$ mm^3, with the longest dimension parallel to [100] prepared at the MPI Institut für Metallforschung of Stuttgart. They were annealed at 2070 K for 8 min at $<10^{-7}$ mbar. Charging with H and D was made by equilibration with appropriate amounts of H_2/D_2 at ~870 K in a UHV system with starting pressure around $10^{-10}-10^{-9}$ mbar. When dealing with such low impurity contents, it is

*Corresponding author. Tel.: +39-06-4993-4114; fax: +39-06-2066-0061.
E-mail address: cordero@idac.rm.cnr.it (F. Cordero).

0925-8388/02/$ – see front matter
doi:10.1016/S0925-8388(02)01268-9

important to check that unwanted oxygen does not affect the measurements, since Nb has a high affinity for O, which in turn forms complexes both with H/D and Zr. This was done in several ways: the resistivities of the $Nb_{1-x}Zr_x$ bars were found in perfect agreement with the nominal Zr contents; the charging and outgassing treatments were verified to not introduce appreciable amounts of O from the reproducibility of the anelastic spectra after several treatments. Finally, it was checked that none of the features of the anelastic spectra is attributable to complexes containing O, by intentionally doping with O.

The samples were suspended in correspondence with the nodal lines and electrostatically excited on their flexural, extensional or torsional modes at frequencies $\omega/2\pi$, measuring the complex dynamic compliance $s(\omega, T) = s' + is''$. The elastic energy dissipation coefficient $Q^{-1} = s''/s'$ was measured from the decay of the free sample vibration, and contains contributions from any dynamic process coupled with the strain caused by the vibration. In the simple case of transitions between two levels E_1 and E_2 modulated by the strain ε according to $\gamma_\alpha = \partial E_\alpha/\partial\varepsilon$ and with instantaneous populations n_α reaching equilibrium with a relaxation rate $\tau^{-1} = \nu_{12} + \nu_{21}$, it is [6]

$$Q^{-1} \simeq \frac{c}{v_0}\frac{n_1 n_2}{k_B T}\frac{(\gamma_1-\gamma_2)^2}{s'}\frac{\omega\tau}{1+(\omega\tau)^2}, \quad (1)$$

peaked at the temperature where $\omega\tau = 1$. In the case of a FLS, the solution of the rate equations would yield much more complicated expressions in terms of n_α and $\nu_{\alpha\beta}$. Still, the relaxation strength (the part independent of $\omega\tau$) is the sum over all the pairs of levels of terms like that in Eq. (1) [7], while it will be shown later that there are mainly two relaxation modes with widely different rates, so that Eq. (1) can be used to discuss the absorption peaks resulting from each of these modes.

3. Results and discussion

3.1. Anelastic spectra at low concentrations of impurities

The anelastic spectra of the hydrogenated substitutional Nb alloys contain contributions from both transitions of H between coherent tunneling states at liquid He temperatures, and from hopping among tunnel systems around a same S atom at liquid N_2 temperatures. The spectra for S concentrations above 0.5 at% display a rather complex phenomenology, which has been in part already discussed [4,8–11] and will not be considered here. We will limit ourselves to the evolution of the spectrum of $Nb_{1-x}Zr_xD_y$ for $x \leq 0.5\%$, as shown in Fig. 1a for the case of the excitation of the 1st extensional mode of [100] oriented samples ($1/2\ (s_{11} - s_{12})$ or E-type mode assuming no pure volume relaxation, $\omega/2\pi \simeq 40$ kHz). Curve 1 refers to the

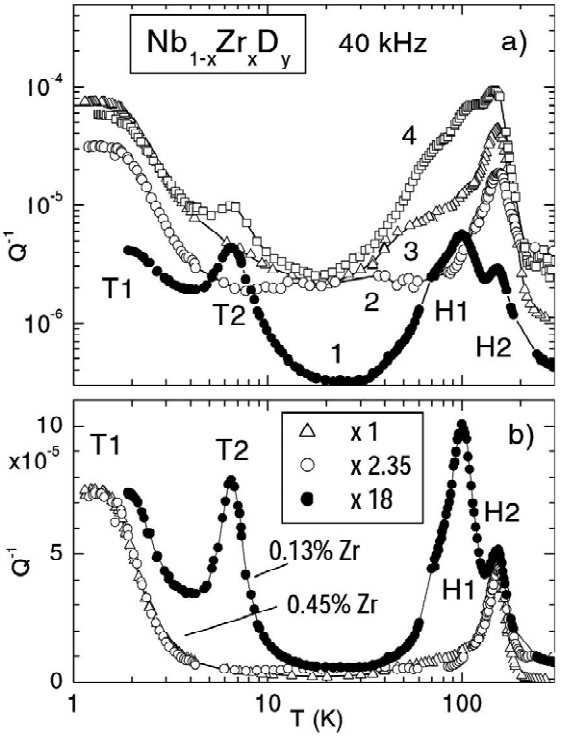

Fig. 1. Evolution of the anelastic spectrum with increasing Zr and D contents; curve 1 refers to the 0.13% Zr sample with 0.015% D, while curves 2 − 4 to the sample with 0.45% Zr and 0.0156%, 0.0353% and 0.14% D. The crystals were excited at $\omega/2\pi \simeq 40$ kHz in extension along [100]. Note that curve 2 has a higher background dissipation. In part b) the curves are normalized to the height of peak H2, multiplying by the factors indicated in the legend. The spectra at low D content y scale with y on the same sample.

sample with 0.13% Zr and 0.0150% D, while curves 2–4 refer to the sample with 0.45% Zr charged with 0.0156%, 0.0363% and 0.14% D, respectively. There are at least four $Q^{-1}(T)$ peaks: the ones labeled T1 and T2, at 2 and 7 K, are due to transitions of the D atoms between coherent tunneling states, while H1 and H2 near 100 and 150 K are due to reorientational hopping around Zr. There is a qualitative change of the spectrum passing from curve 1 at $x = 0.13\%$ to curve 2 at 0.45% with the same $y = 0.015\%$, and the spectrum at $x = 0.13\%$ is certainly more representative of the undistorted Zr–D pairs. Therefore, peaks T2 and H1 are associated with nearly undistorted Zr–D pairs, and this is better seen in Fig. 1b, where the curves are normalized to the intensity of peak H2; it appears that at infinite Zr dilution only peaks T2 and H1 would be present. Instead, processes T1 and H2 must be associated with Zr–D pairs whose symmetry is lowered by the elastic interactions with the other complexes.

It is noteworthy that when passing from curve 1 to curve 2 both peaks T2 and H1 are not broadened or covered by the rest of the spectrum, but they are actually depressed; in addition, peak T2 reappears in the 0.45% Zr sample with practically the same shape with further increase of the D content (curve 4). This behavior can be understood as

follows: the 'little perturbed' Zr–D pairs giving rise to peaks T2 and H1 must have site energy perturbations a (asymmetries) smaller than a value a_0. With 0.13% Zr the width of the distribution $g(a)$ of the energy asymmetries is of the order of a_0, so that there is a considerable fraction of 'little perturbed' Zr–D and peaks T2 and H1 dominate the spectrum. Taking into account the asymmetries found for the TLS of O–H pairs in Nb [1,2], and assuming that substitutional Zr perturbs the lattice much less than interstitial O, it should be $a_0 \sim a(y = 0.13\%) \sim 1 - 5$ K. At higher Zr content, $g(a)$ is broader, and the fraction of sites with $a < a_0$ is correspondingly smaller. Keeping y constant, the total number of complexes with $a < a_0$ may decrease both because of a reduction of the absolute number of Zr atoms whose environment satisfies $a < a_0$, but also because certain types of highly distorted Zr environments may become energetically favorable and therefore more populated by D during cooling. A quantitative estimate of these effects is beyond our possibilities, but an increase of the width of a lorentzian $g(a)$ from e.g. ~1 K to ~10 K would be sufficient to account for a sensible reduction of the intensities of the peaks. Such intensities recover by further increasing y, up to populating again a sufficient number of 'unperturbed' Zr traps, as is particularly evident for peak T2. The fact that its shape remains unaltered demonstrates that it is indeed due to unperturbed traps.

The above explanation is based on the hypothesis that the distribution of asymmetries is only determined by the content x of Zr, while the interaction between D atoms is negligible. This hypothesis is reasonable for $y \ll x$, as in the present experiments, and is confirmed by the fact that the curves 2 and 3 in Fig. 1b, normalized according to the height of peak H2, are nearly coincident, and the normalization factor exactly coincides with the ratio of the D contents y.

3.2. Symmetry of the S–H pair

Fig. 2 represents a Nb cell containing an S atom, with the proposed [8,10] FLS geometry for H delocalization over a cube face. In the unperturbed case, such an S–H pair has a [100] tetragonal symmetry, as is evident by imagining that H is delocalized with the same probability over the four T sites, and this symmetry should appear also in the stress-type dependence of the intensity of the peaks due to the reorientational hopping among different tunnel systems around the S atom (peaks H1 and H2). This is shown in Fig. 3 for the [100] oriented sample with 0.45% Zr, excited on the 1st extensional mode (E-type, $1/2(s_{11} - s_{12})$) and 3rd torsional mode (T-type, s_{44}). Since both modes happen to have nearly the same frequency ~40 kHz, the curves can be directly compared, and it appears that peak H2 is present in the E-type but not in the T-type mode. This becomes clear comparing the E spectrum with the T spectrum multiplied by 3.13 (dashed–dotted line). The absence of peak H1 in the T-type mode demonstrates the tetragonal symmetry of the nearly unperturbed Zr–D pair.

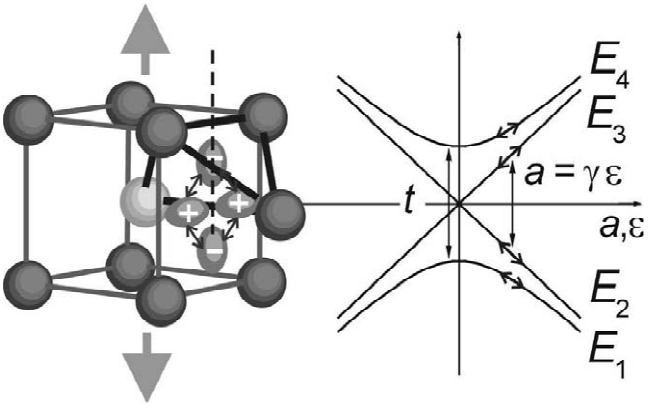

Fig. 2. Cell with a substitutional atom in the center and H delocalized over four tetrahedral sites; each site is surrounded by a tetrahedron of host atoms. The ellipsoids represent the strain tensor (elastic dipole) associated with the H occupation in each site. An E-type strain ε, like that indicated by the arrows, changes the site energies by $\pm a/2$, as indicated by the signs within the ellipsoids. On the right side is the resulting diagram of the energy levels $E_i(\varepsilon)$; the small arrows indicate the modulation of the energies from the strain due to the sample vibration.

It is also interesting to note that the whole spectrum is at least three times less intense under T-type excitation than under the E-type one (20 times smaller at liquid He temperatures [11]), and this is an indication that the H atom feels mainly the tetragonal symmetry of the T site also when trapped by Zr. In fact, the elastic energy of T sites is unchanged by ε_{44} strain [6], and a relaxation of s_{44} can only come from a deviation of the site (or complex) symmetry from the tetragonal one. The fact that the T site symmetry is little affected by the presence of a nearest neighbor substitutional atom is also deduced from the INS spectra of the vibrations of H trapped by substitutional Ti

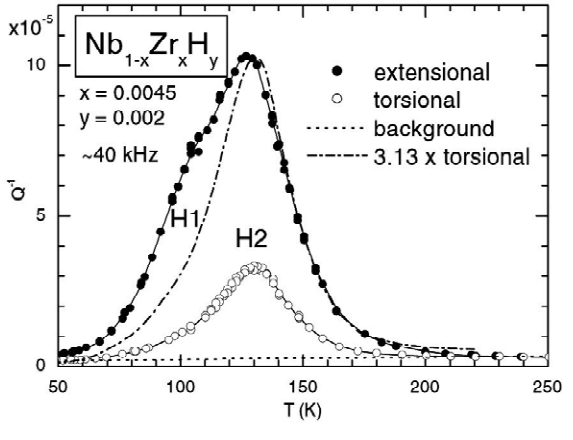

Fig. 3. Dependence of the elastic energy loss on the stress symmetry, by exciting a same [100] oriented crystal on its 1st extensional (E-type) or 3rd torsional (T-type) modes; the frequency is ~40 kHz in both cases, so that the spectra can be directly compared.

in Nb, which are hardly different from those in pure Nb [12].

The distorted pairs responsible for H2 have a lower symmetry and therefore appear also in the s_{44} mode, and they are responsible for the anelastic results on $Nb_{0.98}Ti_{0.02}H_y$, interpreted in terms of jumps between tunnel systems over pairs of T sites across two cube faces with [110] orthorhombic symmetry [4]. Delocalization over a ring of six T sites [5] can be excluded, since it would have [111] symmetry with a dependence of the intensity of peaks H1 and H2 on the stress symmetry opposite to the observed one at all defect concentrations.

3.3. The four-level tunnel system

From the above discussion we conclude that it is possible to approximate the response of a nearly unperturbed FLS in terms of the elastic energy of unperturbed T sites, and therefore it is sufficient to deal with the E-type stress only. In fact, any stress of a cubic crystal can be expressed in terms of hydrostatic, two E-type and three T-type stresses; the latter do not affect the T site energies, while the hydrostatic stress affects all the sites in the same manner. Fig. 2 represents the effect of a uniaxial [100] stress on a FLS; also indicated is the tetrahedron of metal atoms nearest neighbor to a T site, with the tetragonal axis as a dashed line. The pairs of opposite sites indicated with the minus sign have equivalent tetrahedra (a translation and an inversion do not change the strain ellipsoid, neglecting the influence of the S atom) and therefore are elastically equivalent; the other pair of sites indicated with the plus sign have instead tetrahedra rotated by 90°. Then, in the presence of the uniaxial strain the elastic energies of the pairs of sites change by $\pm a/2 = \gamma\varepsilon$, so that the FLS remains centrosymmetric, at least in first approximation. The corresponding Hamiltonian in the localized representation is [1,10]

$$H = \frac{1}{2}\begin{bmatrix} a & t & 0 & t \\ t & -a & t & 0 \\ 0 & t & a & t \\ t & 0 & t & -a \end{bmatrix}, \quad (2)$$

where t is the tunneling matrix element between nn sites, which should be similar to that for tunneling near an O atom [1,2], $t_H/k_B \simeq 2$ K and $t_D/k_B \simeq 0.24$ K with $\partial t/\partial\varepsilon \ll \gamma$, and a is due to the E-type component of a static strain from the surrounding complexes. Two of the eigenstates of Eq. (2) are

$$|1,4\rangle = \frac{1}{2\sqrt{E}}\begin{bmatrix} \sqrt{E \mp a} \\ \mp\sqrt{E - a} \\ \sqrt{E \mp a} \\ \mp\sqrt{E - a} \end{bmatrix}, \quad (3)$$

separated in energy by $E = \sqrt{a^2 + 4t^2}$, and correspond to the levels of a TLS between one of the pairs of nn T sites, but with tunneling energy $2t$ instead of t. When the sample vibration modulates ε, the modulation of E is $\partial E/\partial\varepsilon = (a/E)\gamma$ (indicated by small arrows in Fig. 2) and vanishes for $a = 0$, implying vanishing relaxation strength in Eq. (1), exactly like a TLS. The two intermediate states are

$$|2\rangle = \frac{1}{\sqrt{2}}\begin{bmatrix} 0 \\ 1 \\ 0 \\ -1 \end{bmatrix}, \quad |3\rangle = \frac{1}{\sqrt{2}}\begin{bmatrix} 1 \\ 0 \\ -1 \\ 0 \end{bmatrix} \quad (4)$$

with H delocalized over either of the two pairs of opposite sites with the same energy $\pm a/2$; the resulting energies are therefore $E_{2,3} = \pm a/2$. These levels behave as the classical site energy and the corresponding relaxation strength remains finite also for zero asymmetry. The resulting scheme of the energy levels versus strain is shown in Fig. 2; the introduction of a tunneling matrix element between opposite sites would slightly shift the relative position of the energy levels, leaving unchanged the main features.

3.4. Peak T2: intermediate levels of a FLS

The presence of the two intermediate states 2 and 3 in the energy level scheme of Fig. 2 allows a FLS to be clearly distinguished from a TLS by decreasing the concentration of S atoms, so that the average internal strains become low enough that for a considerable fraction of FLS it is $a \lesssim t$. In fact, in these conditions, the intensity of the tunneling peaks should vanish for TLS but not for FLS. This is just observed in Fig. 1, where passing from 0.45% Zr to 0.13% Zr with the same 0.015% of D, peak T1 decreases 7.7 times, while peak T2 even increases (the increase has been explained in terms of the number of little perturbed Zr–D pairs, see Section 3.1).

Peak T1 is instead due to transitions between levels depending on strain as levels 1 and 4 of a FLS or those of a TLS, and in fact it can be semiquantitatively explained in that way, with parameters of the TLS/FLS close to those of the O–H/D pair [11] (see later). It is even possible to explain a remarkable effect of the isotope mass, with the intensity of D ~50 times larger than that of H [11].

3.5. Dynamics of a FLS

The fact that peak T2 is markedly shifted to higher temperature with respect to H1 implies a much slower relaxation rate. However, even in the case that peak T1 is exclusively due to TLS from very distorted Zr–D pairs and H2 to FLS, if the parameters of FLS and TLS are similar one would expect also similar relaxation rates. Then, it has to be explained why the relaxation of the intermediate levels of a FLS is much slower than that of the levels 1/4 or of a TLS.

The issue of the dynamic response of a FLS is more complex than for a TLS, especially if taking into account the non adiabatic interaction with the conduction electrons [1–3]. An attempt in this sense has recently been done

[13], finding two types of oscillations of the probabilities of the site occupations; long-lived oscillations of H between opposite sites are found even in the incoherent regime, but their decay does not seem slow enough to justify the observed shift of peak T2. Note, however, that the tunneling peaks occur in the superconducting state of Nb ($T_c = 9.25$ K), where the coupling constant $K \simeq 0.07$ to the conduction electrons is reduced by a factor of $2/[1 + \exp(-\Delta/k_B T)]$, $\Delta(T) \simeq \sqrt{1-(T/T_c)^2} \times 17.7$ K being the superconducting energy gap [2,3]. This means that the predominant interaction with the electrons is drastically reduced, and we can use simple perturbation theory between coherent tunneling states. The transition rate between levels i and j is then proportional to $|\langle i|V|j\rangle|^2$, where V is the modulation of the asymmetry a from the interaction with the phonons and the conduction electrons. The transitions between the levels 1 and 4 involve the same matrix element as in the case of TLS between pairs of nn T sites, and therefore the resulting rate is comparable to that of the corresponding TLS. These transitions can contribute to peak T1, together with the relaxation of TLS from very distorted traps. Instead, the matrix element $\langle 2|V|3\rangle$ between the intermediate eigenstates is null, whatever the form of V (but always diagonal). The perturbation V can connect the intermediate levels with levels $1/4$ only if it is non-centrosymmetric; such a perturbation is certainly smaller than the centrosymmetric one, since it is due to the deviations from the perfect lattice introduced by the S atom; the reduction of the intensity of peak T1 by a factor ~ 20 when passing from E-type to T-type excitation demonstrates that such deviations are small [11].

We conclude that first order transitions involving intermediate states of a centrosymmetric FLS are prohibited or occur at a reduced rate due to a matrix element which is null or smaller than $\langle 1|V|4\rangle$; then it is possible that two-phonon and higher order transitions become predominant. This is confirmed by the analysis of peak T2 (Fig. 4a), which can be very well described by $\tau^{-1} \propto T^n$ with $n = 5.4 - 6$ without any broadening. The data of T2 measured in the 0.13% Zr sample with 0.015% D at two frequencies exclude the dependence

$$\tau^{-1} = (\pi/2\hbar)K[1 + \exp(\Delta_s/T)]^{-1}(t/E)^2 4T \qquad (5)$$

expected for transitions promoted by the interaction with the electrons [1,2], and valid for peak T1; on the other hand, the $\tau^{-1} \propto T^n$ dependence, with $n > 2$, is characteristic of two-phonon processes. Fig. 4b shows the same peak measured with H, which again can be remarkably well fitted with the same temperature dependence. The higher background dissipation with the distinct drop below T_c indicates a stronger contribution from transitions promoted by the electron interaction, compared to the D case. The ratio of the relaxation rates of the two isotopes turns out to be $\tau_H^{-1}/\tau_D^{-1} \sim 30$, and since τ^{-1} is proportional to the square of the effective tunneling matrix element, the ratio

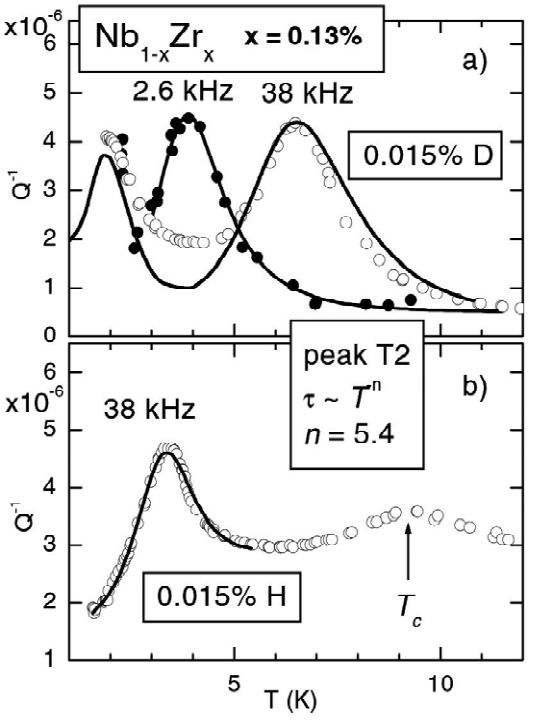

Fig. 4. The two well separated elastic energy loss peaks due to: (i) the relaxation between levels 1 and 4 of FLS and possibly of TLS from distorted Zr–D pairs (peak T1 at 2 K); (ii) the relaxation of the intermediate levels of the FLS (peak T2). The continuous line is obtained assuming 1st order transitions between the levels with interaction with the electrons for peak T1 and a $\tau^{-1} \sim T^{5.4}$ law for peak T2.

of the latter is $t_H/t_D \simeq 5.6$, close to the ratio $7.5 - 9$ found for the TLS of the O–H pair in Nb.

In the higher frequency curve with D we also included the theoretical curve for TLS relaxation with tunneling energy $t_D = 0.12$ K, asymmetries distributed according to a lorentzian of width 2 K, a phonon coupling $\gamma = 500$ K and a rate given by Eq. (5) with $K = 0.07$; these parameters are close to those found for the O–D pair in Nb, and reproduce reasonably well peak T1. Note that the introduction of the distribution function for the asymmetries is essential for the description of peak T1, whose amplitude vanishes for zero asymmetry, but not for T2; the fact that peak T2 does not require the introduction of a broadening, and its shape remains unchanged at higher concentrations (curve 4 of Fig. 1a) is a further confirmation that it is due to nearly unperturbed Zr–D pairs.

4. Conclusion

It is possible to provide a semiquantitative description of the tunneling dynamics of H/D trapped by substitutional Zr in Nb at very low concentrations of Zr and H, when the site energy perturbations due to the elastic interactions do not destroy the symmetry of the S–H pair. The tunneling energy of H and D and the coupling strengths to the

phonons and electron excitations are close to those found for the TLS formed by the O–(H/D) pairs in Nb, indicating that the trapping impurity has a minor role in determining such parameters. The higher symmetry of the Zr–H pair, however, allows H to be delocalized over four tetrahedral sites of a face of the cube containing the substitutional atom, giving rise to a pair of additional eigenstates with respect to a TLS. Such intermediate eigenstates have H delocalized over either pair of equivalent opposite sites, and are clearly revealed thanks to their properties completely different from those of the TLS states. Their energy coincides with that of the pair of equivalent sites without the tunnel splitting contribution, yielding finite relaxation strength also for a completely symmetric FLS; in addition, their symmetry is such that first order transitions between themselves or to the other states are prohibited for nearly undistorted FLS, since they require non-centrosymmetric perturbations. These features manifest themselves in the anelastic response as two distinct relaxation processes at liquid He temperature: one is closely similar to the relaxation of a TLS between nearest neighbor tetrahedral sites, like for the O–H pair, and can be due to the relaxation of both TLS arising from highly distorted Zr–H pairs and levels 1 and 4 of FLS. The second peak is due to the transitions involving the intermediate levels of the FLS and is particularly evident at very low defect concentrations due to the non-vanishing relaxation strength for symmetric tunnel systems. In addition, it is shifted to higher temperature with respect to the TLS-like relaxation and clearly indicates a power law dependence of the relaxation rate on temperature, with exponent $5.4 - 6$, for both H and D isotopes; this is consistent with the suppression of the first order phonon and electron excitations of the intermediate levels, and a residual contribution from higher order phonon transitions.

Acknowledgements

The authors are grateful to H. Schultz for supplying the $Nb_{1-x}Zr_x$ single crystals.

References

[1] P. Esquinazi, Tunneling Systems in Amorphous and Crystalline Solids, Springer, Berlin, 1998.
[2] H. Wipf, in: H. Wipf (Ed.), Hydrogen in Metals III. Properties and Applications, Springer, Berlin, 1997.
[3] U. Weiss, Quantum Dissipative Systems, World Scientific, Singapore, 1999.
[4] O. Yoshinari, K. Tanaka, H. Matsui, Phil. Mag. A 74 (1996) 495.
[5] B. Hauer, R. Hempelmann, D. Richter, T.J. Udovic, J.J. Rush, S.M. Bennington, A.J. Dianoux, Physica B 226 (1996) 210.
[6] A.S. Nowick, B.S. Berry, Anelastic Relaxation in Crystalline Solids, Academic Press, New York, 1972.
[7] F. Cordero, Phys. Rev. B 47 (1993) 7674.
[8] G. Cannelli, R. Cantelli, G. Vertechi, Appl. Phys. Lett. 39 (1981) 832.
[9] G. Cannelli, R. Cantelli, F. Cordero, J. Phys. F: Metal Physics 16 (1986) 1153.
[10] G. Cannelli, R. Cantelli, F. Cordero, F. Trequattrini, Phys. Rev. B 49 (1994) 15040.
[11] G. Cannelli, R. Cantelli, F. Cordero, F. Trequattrini, H. Schultz, J Alloys Comp. 231 (1995) 274.
[12] D. Richter, J.J. Rush, J.M. Rowe, Phys. Rev. B 27 (1983) 6227.
[13] M. Winterstetter, M. Grifoni, Phys. Rev. B 62 (2000) 3237.